DEUTSCHES ELEKTRONEN-SYNCHROTRON

DESY 94-110
July 1994

Determination of the Radiative Decay Width of the η_c Meson

The ARGUS Collaboration

ISSN 0418-9833

NOTKESTRASSE 85 - 22603 HAMBURG

To be sure that your preprints are promptly included in the
HIGH ENERGY PHYSICS INDEX,
send them to (if possible by air mail):

DESY	**DESY-IfH**
Bibliothek	**Bibliothek**
Notkestraße 85	**Platanenallee 6**
22603 Hamburg	**15738 Zeuthen**
Germany	**Germany**

DESY 94-110
July 1994

ISSN 0418-9833

Determination of the Radiative Decay Width of the η_c Meson

The ARGUS Collaboration

H. Albrecht, T. Hamacher, R. P. Hofmann, T. Kirchhoff, R. Mankel[1], A. Nau, S. Nowak[1], D. Reßing, H. Schröder, H. D. Schulz, M. Walter[1], R. Wurth
DESY, Hamburg, Germany

C. Hast, H. Kapitza, H. Kolanoski, A. Kosche, A. Lange, A. Lindner, M. Schieber, T. Siegmund, B. Spaan, H. Thurn, D. Töpfer, D. Wegener
Institut für Physik[2], Universität Dortmund, Germany

P. Eckstein, M. Schmidtler, M. Schramm, K. R. Schubert, R. Schwierz, R. Waldi
Institut für Kern- und Teilchenphysik[3], Technische Universität Dresden, Germany

K. Reim, H. Wegener
Physikalisches Institut[4], Universität Erlangen-Nürnberg, Germany

R. Eckmann, H. Kuipers, O. Mai, R. Mundt, T. Oest, R. Reiner, W. Schmidt-Parzefall
II. Institut für Experimentalphysik, Universität Hamburg, Germany

J. Stiewe, S. Werner
Institut für Hochenergiephysik[5], Universität Heidelberg, Germany

K. Ehret, W. Hofmann, A. Hüpper, K. T. Knöpfle, J. Spengler
Max-Planck-Institut für Kernphysik, Heidelberg, Germany

P. Krieger[6], D. B. MacFarlane[7], J. D. Prentice[6], P. R. B. Saull[7], K. Tzamariudaki[7], R. G. Van de Water[6], T.-S. Yoon[6]
Institute of Particle Physics[8], Canada

C. Frankl, M. Schneider, S. Weseler
Institut für Experimentelle Kernphysik[9], Universität Karlsruhe, Germany

G. Kernel, P. Križan, E. Križnič, T. Podobnik, T. Živko
Institut J. Stefan and Oddelek za fiziko[10], Univerza v Ljubljani, Ljubljana, Slovenia

V. Balagura, I. Belyaev, S. Chechelnitsky, M. Danilov, A. Droutskoy, Yu. Gershtein, A. Golutvin, I. Korolko, G. Kostina, D. Litvintsev, V. Lubimov, P. Pakhlov, S. Semenov, A. Snizhko, I. Tichomirov, Yu. Zaitsev
Institute of Theoretical and Experimental Physics, Moscow, Russia

[1] DESY, IfH Zeuthen
[2] Supported by the German Bundesministerium für Forschung und Technologie, under contract number 054DO51P.
[3] Supported by the German Bundesministerium für Forschung und Technologie, under contract number 056DD11P.
[4] Supported by the German Bundesministerium für Forschung und Technologie, under contract number 054ER12P.
[5] Supported by the German Bundesministerium für Forschung und Technologie, under contract number 055HD21P.
[6] University of Toronto, Toronto, Ontario, Canada.
[7] McGill University, Montreal, Quebec, Canada.
[8] Supported by the Natural Sciences and Engineering Research Council, Canada.
[9] Supported by the German Bundesministerium für Forschung und Technologie, under contract number 055KA11P.
[10] Supported by the Ministry of Science and Technology of the Republic of Slovenia and the Internationales Büro KfA, Jülich.

Abstract

An analysis of the reaction $\gamma\gamma \to \eta_c$ was performed in five different decay channels of the η_c: $K^0_S K^\pm\pi^\mp$, $K^+K^-\pi^+\pi^-$, $2\pi^+2\pi^-$, $\phi\phi$ and $2K^+2K^-$. A value $\Gamma_{\gamma\gamma}(\eta_c) = (11.3 \pm 4.2)$ keV was obtained for the radiative decay width by combining the results from the first four channels. Using our result on the two-photon width we also determined the branching ratio for the decay $\eta_c \to 2K^+2K^-$.

The measurements of the radiative decay widths of hadrons have proved to be one of the most important tools to study the composition and the properties of the bound states of strong interactions. While for light quarks the understanding of the binding forces is still on a more phenomenological level, in heavy quark systems, such as charmonium, fundamental tests of QCD dynamics can be made. One of the important quantities in the charmonium system is the relation between the leptonic decay width of the J/ψ and the two-photon width of the η_c which is to the lowest order given by (see for example [1])

$$\frac{\Gamma_{\gamma\gamma}(\eta_c)}{\Gamma_{e^+e^-}(J/\psi)} = 3e_Q^2\left(\frac{M_{J/\psi}}{M_{\eta_c}}\right)^2.$$

QCD corrections have been calculated to order α_s by Barbieri et al. [2] resulting in the relation $\Gamma_{\gamma\gamma}(\eta_c) = \Gamma_{e^+e^-}(J/\psi)\cdot(1.60^{+0.07}_{-0.05})$, which, together with $\Gamma_{e^+e^-}(J/\psi) = (5.36 \pm 0.29)$ keV [3], yields the prediction $\Gamma_{\gamma\gamma}(\eta_c) = (8.6 \pm 0.6)$ keV. Furthermore, with the assumption that the hadronic η_c decays can be described by the lowest order two-gluon diagram one obtains the ratio of the hadronic to two-photon partial width $\Gamma_{\mathrm{hadrons}}(\eta_c)/\Gamma_{\gamma\gamma}(\eta_c)$ proportional to $(\alpha_s/\alpha)^2$. This relation could in principle be used to determine α_s. However, in this case the QCD radiative corrections seem to be too large to provide a reliable prediction.

The radiative decay width $\Gamma_{\gamma\gamma}(\eta_c)$ has been measured by two different methods: in photon-photon collision experiments [4-7] and by the measurement of the process $p\bar{p} \to \gamma\gamma$ [8]. The most significant results were obtained from the analysis of the decay channel $\eta_c \to K^0_S K^\pm\pi^\mp$, where a good identification of the K^0_S was achieved by determining its decay vertex. The results range from 4 to 27 keV and have large errors because of the small number of collected η_c events and uncertainties in the knowledge of η_c branching ratios. The present analysis aims at improving the precision of the $\Gamma_{\gamma\gamma}(\eta_c)$ measurement by using several decay channels of the η_c meson.

The data used in this analysis were collected using the ARGUS detector at the e^+e^- storage ring DORIS II at DESY, and correspond to an integrated luminosity of 473 pb^{-1}. The beam energies varied between 4.7 and 5.3 GeV. The ARGUS detector and details about its trigger and its particle identification capabilities were described elsewhere [9]. In what follows, we describe the main features of the analysis, while details can be found in refs. [10, 11].

The two-photon production of the η_c was studied in e^+e^- interactions via the reaction

$$e^+e^- \;\to\; e^+e^-\eta_c \qquad (1)$$

with the η_c decaying as follows:

$$\eta_c \rightarrow K_S^0 K^{\pm}\pi^{\mp} \rightarrow \pi^+\pi^- K^{\pm}\pi^{\mp} \quad (2a)$$
$$\eta_c \rightarrow K^+K^-\pi^+\pi^- \quad (2b)$$
$$\eta_c \rightarrow 2\pi^+ 2\pi^- \quad (2c)$$
$$\eta_c \rightarrow \phi\phi \rightarrow 2K^+2K^- \quad (2d)$$
$$\eta_c \rightarrow 2K^+2K^- \quad \text{(including } \phi K^+K^-\text{)}. \quad (2e)$$

We required for the final–state particles to have the vector sum of transverse momenta, $\sum \vec{p_t}$, close to zero and that no other particles were detected, since the final–state electrons scatter predominantly close to the beam direction and escape detection. In this way two-photon processes with almost real photons were selected (no-tag condition).

Candidates for η_c decays (2a) to (2e) were selected from events with four charged particles and zero net charge in the final state. In the case of decays (2b) to (2e) all four particles had to originate from a main vertex close to the nominal interaction point. In the case of decay channel (2a) we have accepted two classes of events. Either two particles with opposite charge had to originate from a common vertex close to the nominal interaction point, while the other two had to form a secondary decay vertex, or all four particles had to fulfil the same conditions for the vertex as in the case of decays (2b) to (2e). In order to use only well measured tracks, we required for each charged particle that the angle θ between the momentum direction and the beam axis fulfilled $|\cos(\theta)| \leq 0.92$, and for the transverse momentum $p_t \geq 0.06$ GeV/c ($p_t \geq 0.13$ GeV/c for the decay channel (2e)).

Particle identification is performed by using data from measurements of specific ionisation and time–of–flight. A normalized likelihood is calculated for each of the mass hypotheses, e, μ, π, K and p [9]. A hypothesis was accepted if the normalized likelihood exceeded a channel specific value from 1% to 25% [10, 11].

Particles associated with the K_S^0 had to be identified as pions, and their invariant mass was required to lie within 20 MeV around the nominal K_S^0 mass (fig. 1), corresponding to about three standard deviations of the Monte Carlo simulated distribution of K_S^0 masses.

The main background reduction came from the condition on the vector sum of the transverse momenta of the detected charged particles, which is for the decays (2a) and (2d) $(\sum \vec{p_t})^2 \leq 0.03$ $(\mathrm{GeV/c})^2$ and for the other decay channels $(\sum \vec{p_t})^2 \leq 0.007$ $(\mathrm{GeV/c})^2$.

A further background reduction was achieved by restricting the number of photons in the event. In the case of the η_c decays (2b) and (2c) no photons were allowed in the final state. Photons were defined as calorimeter hits corresponding to energy deposits of more than 80 MeV, which were not associated with charged tracks. Shower counters with high noise rates were excluded from the analysis. Due to the splitting of showers initiated by charged particles in the calorimeter, parts of the showers can be misinterpreted as photons. Only clusters clearly separated from clusters caused by charged particles were considered as photons. This separation was performed by requiring $|\cos(\vartheta_{c\gamma})| < 0.9$, where $\vartheta_{c\gamma}$ is the angle between the line from the interaction point to the hit in the calorimeter and the line from the interaction point to the point, where the charged track hits the calorimeter. In this way the requirement, that no photons are present in the event, rejected 21% of events corresponding

to channel (2b), and 16% of events corresponding to (2c). In the case of channels (2a) and (2e) up to three photons were allowed in the event, so that the analysis could be done without accounting for noisy shower counters and splitting of showers. The efficiency reduction by this constraint is 1.2%. For the decay channel (2d) no constraint on the number of photons was imposed. These criteria were taken into account when determining the overall acceptance.

In the case of decay (2a) and (2b) several combinations could fulfil the particle hypotheses. If the particle identification was not unique the combination with the highest probability was chosen. From Monte Carlo simulation studies we conclude that with this procedure more than 95% of events were properly identified. The remaining wrong combinations have usually invariant masses close to the η_c mass, leading to small tails in the distribution. The effect was taken into account in the efficiency determination as described below.

With this selection the invariant mass spectra for the channels (2a) to (2c) in fig. 2 were obtained. Figure 3 shows the invariant mass spectra for the four-kaon channels (2d) and (2e). In an attempt to increase the efficiency for these channels the particle identification requirements could be relaxed by exploiting in addition the mass constraint in channel (2d) and the balance of strangeness in (2e). In particular, no particle identification was required for the $\phi\phi$ channel (2d). Candidates for this channel were selected by forming the invariant masses of each pair of oppositely charged particles assuming kaon masses. An event was selected, if it had a combination with both K^+K^- masses within 15 MeV/c^2 of the ϕ mass. No such event with a $\phi\phi$ invariant mass in the η_c region was found (fig. 3).

To select the decay channel (2e) three of the four particles were required to be consistent with the kaon hypothesis and to have a momentum below 1 GeV/c^2. The four kaon mass spectrum in fig. 3b shows a clean η_c peak together with a reflection from channel (2b) around 3.3 GeV/c^2. In the four-kaon channel we also searched for the decay $\eta_c \rightarrow \phi K^+K^-$. Candidate events had to have a K^+K^- combination with an invariant mass within 6 MeV/c^2 of the ϕ mass. Two events were found in the η_c region above no background (fig. 3).

Several possible background contributions in the signal region were considered. The dominant background under the η_c signals is due to the non-resonant two-photon production of the considered final states. Other possible sources of background are the reactions $\gamma\gamma \rightarrow \pi^+\pi^-\pi^+\pi^-\pi^0$ and $\gamma\gamma \rightarrow K^+K^-\pi^+\pi^-\pi^0$, where the π^0 is not observed. This would mainly affect the $\gamma\gamma \rightarrow \pi^+\pi^-\pi^+\pi^-$ and $\gamma\gamma \rightarrow K^+K^-\pi^+\pi^-$ data. Using the published data [12, 13] and Monte-Carlo simulations we find that these two sources contribute 8 events to the channel $\pi^+\pi^-\pi^+\pi^-$ and 7 events to the channel $K^+K^-\pi^+\pi^-$ in the 2.5 GeV to 3.5 GeV region. The background from the reaction $e^+e^- \rightarrow \tau^+\tau^-$ amounts to 2 events in the whole 2.5 GeV to 3.5 GeV invariant–mass region for the channel $\pi^+\pi^-\pi^+\pi^-$, while this contribution is almost negligibile for the other channels. The sum of the above mentioned non-two-photon background contributions amounts to 2% of all accepted events in the 2.5 GeV to 3.5 GeV region for the channels $\pi^+\pi^-\pi^+\pi^-$ and $K^+K^-\pi^+\pi^-$. Independently, one can check the total amount of non-two-photon background by comparing the simulated $(\sum \vec{p_t})^2$ distribution to the measured one. We conclude that this kind of background cannot exceed 4%. Monte Carlo studies show that all of the discussed background sources have a smooth behaviour in the signal region and thus do not contribute to the number of η_c's as determined by the fit.

Another source of background is due to particle misidentification which leads to a reflection of one channel into the others. Most of the reflected spectrum is a slowly varying function of the invariant mass and is treated together with the continuum part of the channel spectrum. On the other hand, the main resonance structure that can be reflected is the η_c itself. Monte Carlo studies show that such misidentified η_c events follow a Gaussian-like distribution. For example: between the events which were accepted as $\gamma\gamma \to K^+K^-\pi^+\pi^-$, we expect to find events coming from the channel (2c) centered at 3.20 GeV, with $\sigma = 35$ MeV. Using the known values for η_c branching ratios, the expected number of misidentified events coming from (2c) is 22% of properly identified events coming from (2b).

The shapes of the η_c mass distributions and the acceptances were determined by a Monte Carlo simulation of the two-photon production of the η_c according to reaction (1) and subsequent decays into channels (2a) to (2e). The decays were generated according to uniform phase space distributions, except for channel (2d), where the angular distribution for the decay of a pseudoscalar into two vector mesons was taken into account. The cross section used for the generation of events from reaction (1) was a product of the luminosity function for transverse photons [14] and a two-photon cross section, which contains a relativistic Breit-Wigner function for the η_c production ($M_{\eta_c} = 2.979$ GeV, $\Gamma_{\eta_c} = 10.3$ MeV [3]) and a J/ψ form factor for each photon to account for the virtuality of the photons. Since the virtuality of the two photons is restricted by the $(\sum \vec{p_t})^2$ cut, the results were insensitive to the chosen form factors, e.g. a ρ form factor changes the result for the radiative width by less than 1% for $(\sum \vec{p_t})^2 < 0.03\ (\mathrm{GeV}/c)^2$.

The Monte Carlo generated events were passed through the detector simulation program, and were reconstructed and selected using the same programs as for the data. The trigger simulation used thresholds for the detector components as determined from the data. The overall acceptance after applying the cuts amounted to 8.7 % for channel (2a), 7.9 % for (2b), 11.6 % for (2c), 10.7 % for (2d) and 5.6 % for (2e) with a J/ψ form factor. According to the simulation the η_c signal for the measured channels can be described by a Gaussian function with σ ranging from 15 to 25 MeV.

The number N_i of accepted η_c events in the channel i has been determined by fitting the spectra in figs. 2 and 3. The fit function was the sum of a Breit-Wigner folded by a Gaussian for the signal, terms describing reflections of the η_c from the other decay channels, and an exponential function for the background description. The η_c mass was taken from [3] while the width of the distribution was fixed to the simulation results. The reflections were accounted for in the fit by using the Gaussian functions as determined by the Monte Carlo simulation with mass, width and normalisation fixed. The fitted number of η_c's in each channel is given in the second column of table 1 together with the statistical error from the fit. The direct result of the analysis is the product of η_c radiative width with the decay branching ratio for each of the decay channels (table 1). It was calculated using the following formula

$$\Gamma_{\gamma\gamma} \cdot \mathrm{Br}(\eta_c \to i) = \frac{M_{\eta_c}^2}{(2\pi\hbar c)^2} \frac{N_i}{\epsilon_i\ \Lambda\ dL_{\gamma\gamma}^{TT}/dW_{\gamma\gamma}}.$$

The value of the two-photon flux function $dL_{\gamma\gamma}^{TT}/dW_{\gamma\gamma}$ at the η_c mass was determined by a numerical integration of the flux of transverse photons including the same form factors as used in the acceptance calculation. The systematic error on the integrated luminosity Λ

(1.8%) is common to all channels i in the above formula. The systematic error of the fit procedure was estimated to be 3% for channels (2a), (2b) and (2e) and 7% for channel (2c). The main uncertainty comes from the determination of acceptance ϵ_i which is almost equal for all channels, and amounts to 9%.

Several tests have been carried out to check, whether we understand our efficiency determination correctly. The particle identification was tested by varying the likelihood cuts. The photon rejection procedure was checked by varying the number of photons allowed in the event. Finally, in order to test our simulation in total, the selected sample was restricted to the event topologies, in which the measurement conditions are most stable. In all cases the final results were in agreement within statistics.

For each decay channel the two-photon radiative decay width, as listed in the last column of table 1, has been extracted from the measured product $\Gamma_{\gamma\gamma}(\eta_c) \cdot \mathrm{Br}_i$ by dividing through the decay branching ratios. These branching ratios, which are also listed in table 1, have been determined as averages from Mark III and DM2 [15, 16]. The quoted errors take into account that these experiments are correlated due to the common use of the branching ratio of $J/\psi \to \eta_c\gamma$ [1]. In addition, the relation $\mathrm{Br}(\eta_c \to K_S^0 K^\pm \pi^\mp) = 2 \cdot \mathrm{Br}(\eta_c \to K^+K^-\pi^0)$ was used to improve the value for the $K_S^0 K^\pm \pi^\mp$ channel. For the $\phi\phi$ final state, the average from all modes from [16] was taken.

Our final result on the two-photon width of the η_c,

$$\Gamma_{\gamma\gamma}(\eta_c) = (11.3 \pm 4.2)\ \mathrm{keV},$$

was obtained as the weighted average of the first four decay modes. Only uncorrelated errors were considered at this step; the common systematic errors (30%) were added subsequently in quadrature. They include the uncertainty in the branching ratio of the decay $J/\psi \to \gamma\eta_c$ (28%), and the uncertainty in the determination of the acceptance and the luminosity. If we quote the uncertainty of the branching ratio $\mathrm{Br}(J/\psi \to \eta_c\gamma)$ separately as a second error, our result reads

$$\Gamma_{\gamma\gamma}(\eta_c) = (11.3 \pm 2.7 \pm 3.2)\ \mathrm{keV}.$$

In summary, for four different channels of the η_c meson we determined the product of the two-photon width times the branching ratio, $\Gamma_{\gamma\gamma}(\eta_c) \cdot \mathrm{Br}(\eta_c \to X)$, the most significant being $\Gamma_{\gamma\gamma}(\eta_c) \cdot \mathrm{Br}(\eta_c \to K_S^0 K^\pm \pi^\mp) = (0.28 \pm 0.07)$ keV. This value is consistent with the world average of (0.23 ± 0.08) keV. The good particle identification capabilities of our detector made it possible to observe the η_c signal also in channels not containing K_S^0 mesons in the final state. The results for the two-photon width as measured in the different channels are consistent with each other and with previous measurements. Combining the results for channels (2a) to (2d) we obtain $\Gamma_{\gamma\gamma}(\eta_c) = (11.3 \pm 2.7 \pm 3.2)$ keV.

Finally, by using our result on $\Gamma_{\gamma\gamma}(\eta_c)$ we obtain the branching ratio $\mathrm{Br}(\eta_c \to 2K^+2K^-) = 0.021 \pm 0.010 \pm 0.006$. The second error is again the uncertainty originating from the error on the branching ratio of $J/\psi \to \eta_c\gamma$.

[1] Note that in the 1992 Review of Particle Properties [3] the average values for branching ratios were calculated as if the results from the different experiments were not correlated. There is also a numerical error in the listed value for $\mathrm{Br}(\eta_c \to K\bar{K}\pi)$.

Acknowledgement
It is a pleasure to thank U. Djuanda, E. Konrad, E. Michel, and W. Reinsch for their competent technical help in running the experiment and processing the data. We thank Dr. H. Nesemann, B. Sarau, and the DORIS group for the excellent operation of the storage ring. The visiting groups wish to thank the DESY directorate for the support and kind hospitality extended to them.

References

[1] F.E. Close, *An Introduction to Quarks and Partons*, Academic Press, 1979.

[2] R. Barbieri, R. Gatto, E. Remiddi, Phys. Lett. 106B (1981) 497.

[3] Particle Data Group, *Review of Particle Properties*, Phys. Rev. D45 Part II (1992).

[4] PLUTO Coll., C. Berger et al., Phys. Lett. 167B (1986) 120.

[5] TPC/2γ Coll., H. Aihara et al., Phys. Rev. Lett. 60 (1988) 2355.

[6] TASSO Coll., W. Braunschweig et al., Z. Phys. C41 (1989) 533.

[7] CLEO Coll., W.-Y. Chen et al., Phys. Lett. 243B (1990) 169.

[8] R704 Coll., C. Baglin et al., Phys. Lett. 187B (1987) 191.

[9] ARGUS Coll., H. Albrecht et al., Nucl. Instrum. Methods, A275 (1989) 1.

[10] T. Živko, Magistrsko delo - Master thesis, University of Ljubljana, Ljubljana (1991).

[11] A. Lange, Dissertation - Doctoral thesis, University of Dortmund, Dortmund (1993).

[12] ARGUS Coll., H. Albrecht et al., Phys. Lett. 196B (1987) 101.

[13] ARGUS Coll., H. Albrecht et al., Phys. Lett. 210B (1988) 273.

[14] V.M. Budnev et al., Phys. Rep. 15 (1975) 181.

[15] D.Bisello et al., Nucl. Phys. B350 (1991) 1; R.M. Baltrusaitis et al., Phys. Rev. D 33 (1986) 629.

[16] Z. Bai et al., Phys. Rev. Lett. 65 (1990) 1309.

Table 1. Results of the analysis of $\gamma\gamma \to \eta_c$.

If two errors are given, the first error shown is statistical, the second systematical. In the case of results for two-photon width, the first error is statistical, the second uncorrelated systematical, and the third the correlated systematical error. Upper limits correspond to 95 % confidence level.

Channel	Events	$\Gamma_{\gamma\gamma}(\eta_c) \cdot Br_i$ in keV	Br_i [15, 16] in %	$\Gamma_{\gamma\gamma}(\eta_c)$ in keV
$K^0_S K^\pm \pi^\mp$	22.0 ± 5.3	$0.281 \pm 0.068 \pm 0.028$	1.78 ± 0.56	$15.8 \pm 3.8 \pm 2.3 \pm 4.5$
$K^+K^-\pi^+\pi^-$	13.9 ± 6.6	$0.17 \pm 0.08 \pm 0.02$	2.13 ± 0.68	$8.2 \pm 3.9 \pm 1.3 \pm 2.3$
$2\pi^+2\pi^-$	21.4 ± 8.6	$0.18 \pm 0.07 \pm 0.02$	1.09 ± 0.37	$16.7 \pm 6.7 \pm 3.5 \pm 4.6$
$\phi\phi \to 2(K^+K^-)$	< 3.0	< 0.0309	0.171 ± 0.062	<24.1
$2K^+2K^{-a}$	9.1 ± 3.5	$0.231 \pm 0.090 \pm 0.023$	-	-
ϕK^+K^-	< 6.3	< 0.152	-	-

[a] $\eta_c \to 2K^+2K^-$ contains all topological modes except $\eta_c \to \phi\phi$.

Figure Captions

Fig. 1 Invariant mass of $\pi^+\pi^-$ for events in the η_c region (2.90 GeV $< W_{\gamma\gamma} <$ 3.06 GeV) : (a) for events with a secondary vertex, (b) for events without a reconstructed secondary vertex.

Fig. 2 Invariant mass distributions of $K^0_S K^\pm\pi^\mp, 2\pi^+2\pi^-$ and $K^+K^-\pi^+\pi^-$ final states.

Fig. 3 Invariant mass distributions of $\phi\phi, 2K^+2K^-$ and ϕK^+K^- final states.

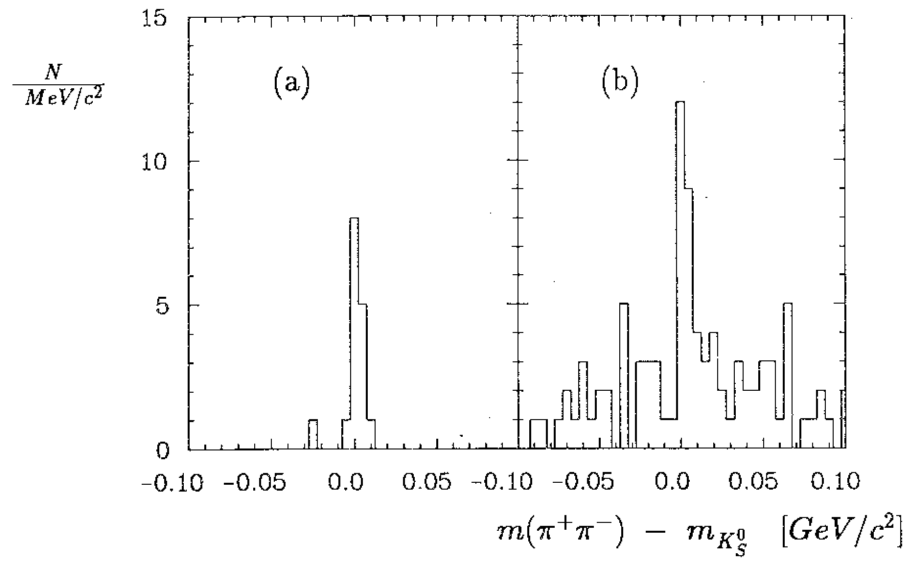

Figure 1:

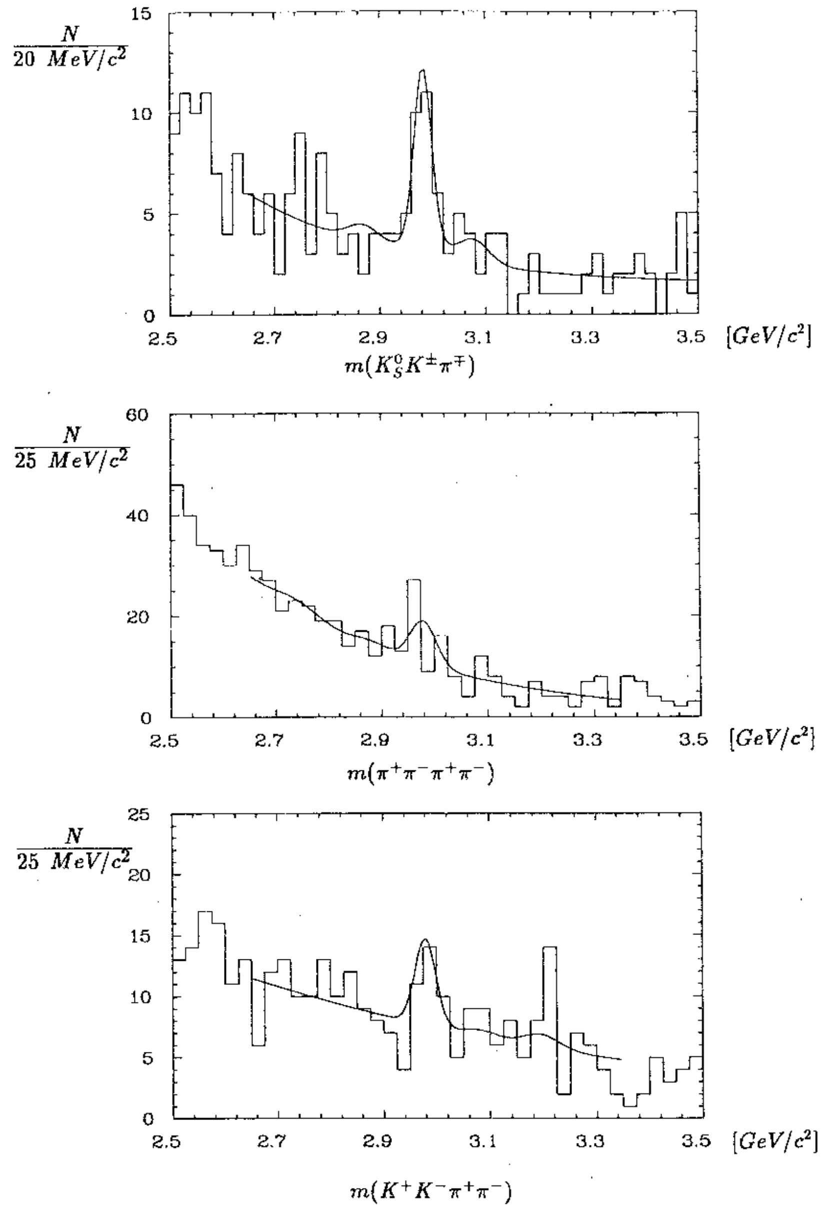

Figure 2:

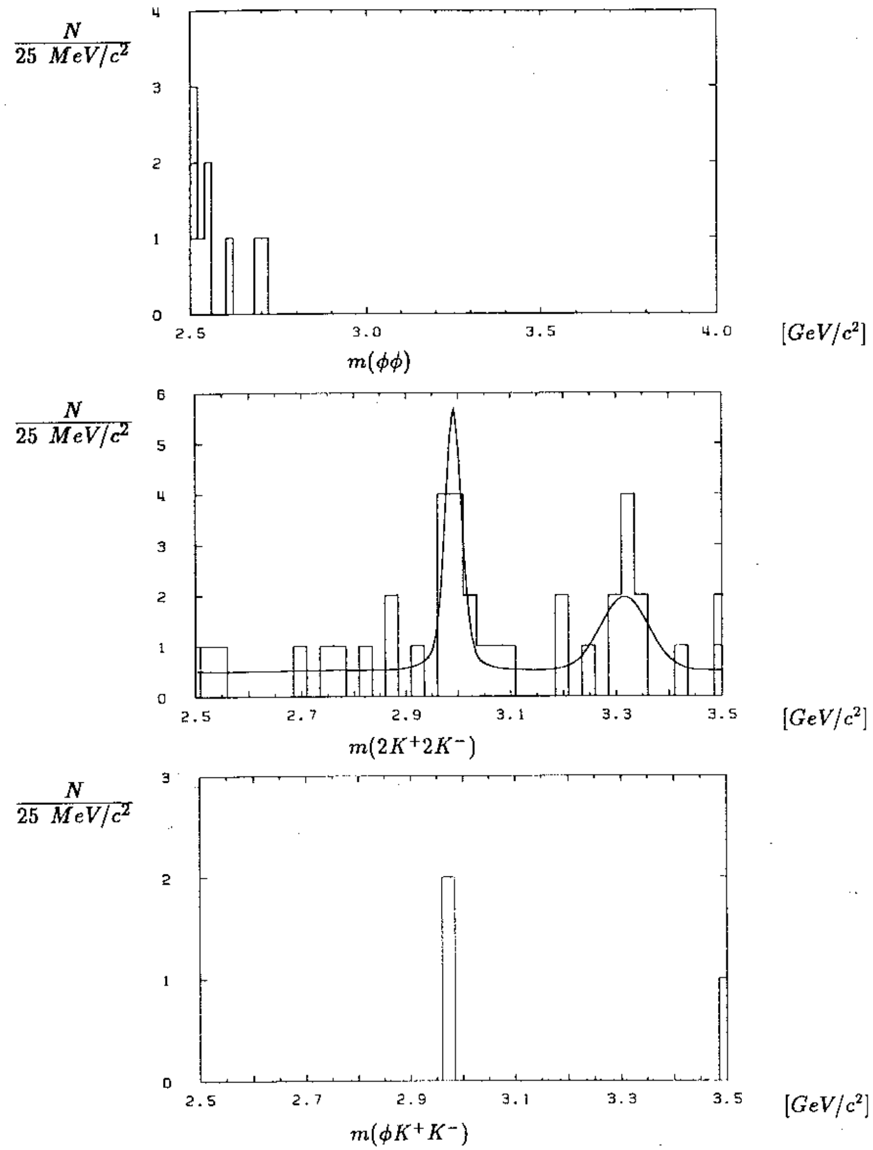

$\frac{N}{25\ MeV/c^2}$
4
3
2
1
0
2.5
3.0
3.5
4.0
$[GeV/c^2]$
$m(\phi\phi)$
$\frac{N}{25\ MeV/c^2}$
6
5
4
3
2
1
0
2.5
2.7
2.9
3.1
3.3
3.5
$[GeV/c^2]$
$m(2K^+2K^-)$
$\frac{N}{25\ MeV/c^2}$
3
2
1
0
2.5
2.7
2.9
3.1
3.3
3.5
$[GeV/c^2]$
$m(\phi K^+K^-)$

Figure 3: